LANGMUIR

Article

pubs.acs.org/Langmuir

Interferences of Silica Nanoparticles in Green Fluorescent Protein Folding Processes

Géraldine Klein,[†,‡] Stéphanie Devineau,[†] Jean Christophe Aude,[‡] Yves Boulard,[§] Hélène Pasquier,[∥] Jean Labarre,[‡] Serge Pin,[†] and Jean Philippe Renault*[,†]

[†]NIMBE, CEA/DSM/IRAMIS et UMR3685 CNRS, CEA-Saclay, Gif sur Yvette, France

[‡]Service de Biologie Intégrative et Génétique Moléculaire, iBiTec-S, FRE3377 CEA-CNRS-Université Paris-Sud, CEA-Saclay, Gif sur Yvette, France

[§]Service de Bioénergétique, Biologie Structurale et Mécanismes, iBiTec-S, UMR 9198 CEA-CNRS-Université Paris-Sud, CEA-Saclay, Gif sur Yvette, France

[∥]Laboratoire de Chimie Physique, UMR 8000, CNRS-Université Paris-Sud, Orsay, France

Supporting Information

ABSTRACT: We investigated the relationship between unfolded proteins, silica nanoparticles and chaperonin to determine whether unfolded proteins could stick to silica surfaces and how this process could impair heat shock protein activity. The HSP60 catalyzed green fluorescent protein (GFP) folding was used as a model system. The adsorption isotherms and adsorption kinetics of denatured GFP were measured, showing that denaturation increases GFP affinity for silica surfaces. This affinity is maintained even if the surfaces are covered by a protein corona and allows silica NPs to interfere directly with GFP folding by trapping it in its unstructured state. We determined also the adsorption isotherms of HSP60 and its chaperonin activity once adsorbed, showing that SiO_2 NP can interfere also indirectly with protein folding through chaperonin trapping and inhibition. This inhibition is specifically efficient when NPs are covered first with a layer of unfolded proteins. These results highlight for the first time the antichaperonin activity of silica NPs and ask new questions about the toxicity of such misfolded proteins/nanoparticles assembly toward cells.

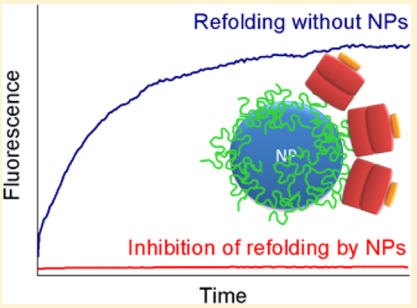

INTRODUCTION

The rapid development of nanomaterials has stirred a renewed interest in protein adsorption phenomena that seem to control nanodrug biodistribution[1] and nanoparticle (NP) toxicity.[2] Many studies support that the function and/or the structure of proteins[3] can be modified through the interaction with NPs. However, the connection between protein adsorption and nanoparticle toxicity remains hard to make, as no specific protein function has been shown to be specifically targeted by nanoparticles up to now.[4] Hundreds of proteins are indeed susceptible to interact with the nanoparticle surfaces, which result in a very small number of each type being really trapped on the nanoobject. This view may be challenged by recent proteomic studies conducted on cellular extracts that, when analyzed from a functional point of view, reveal an over-representation of chaperones among adsorbed proteins (see ref 5 and SI Table S1). This point may be of particular interest, as chaperonin systems are key components of the protein metabolism, assisting in the co and post translational protein folding and the refolding of stressed proteins.[6] Owing to their role in protein folding, chaperons play a role in many pathalogies[7] including neurodegenerative ones.[8] They gain also importance as potential pharmacological targets in cancer therapy.[9] We must finally notice that protein folding processes have been evidenced as being adversely affected by nanoparticles in various in vivo studies.[10−12]

Consequently we conducted a systematic study on the relationships between protein folding, silica NPs action and chaperonin activity. We chose a simple folding process: the refolding of acid-denatured green fluorescent protein (dGFP) by pH jump[13] whose kinetics can be followed by fluorescence even in the presence of nanoparticles (Figure 1). The fluorescence of GFP is very sensitive to the protein folding state, and any misfolding will lead to quenching of light emission. We chose the same silica nanoparticles as the one used for the proteomic studies, that have a nominal size of 26 nm and that have been extensively characterized (see Experimental Section). The chaperonin system used was a complex of Heat Shock Protein 60 and Heat Shock Protein 10 (HSP_{60+10})[14] and is more thoroughly described below.

RESULTS AND DISCUSSION

After a pH jump, the dGFP renaturation can occur either spontaneously or can be catalyzed by HSP_{60+10} (Figure 1). The spontaneous refolding of dGFP leads to a 65% recovery of the

Received: October 20, 2015
Revised: December 6, 2015
Published: December 9, 2015

DOI: 10.1021/acs.langmuir.5b03890
Langmuir 2016, 32, 195−202

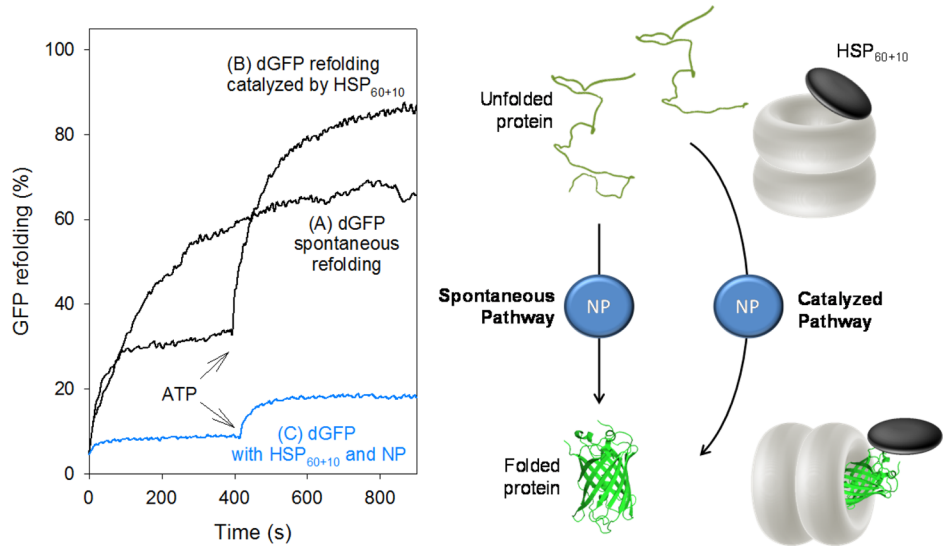

Figure 1. (Left panel) Refolding of acid-denatured GFP (50 nM): (A) spontaneous, (B) mediated by the HSP_{60+10} complex system and (C) mediated by the HSP complex system in the presence of SiO_2 nanoparticles (40 $\mu g\ mL^{-1}$). (Right Panel) Two possible actions of silica nanoparticles to inhibit protein folding: (i) NPs may interfere with protein folding by trapping unfolded proteins in their denatured state (ii) by inhibiting chaperonin catalytic activity.

fluorescence (Figure 1 left panel, trace A). The catalytic action of HSP_{60+10} in the presence of ATP (adenosine triphosphate) allows to achieve 90% of refolding (Figure 1, trace B) but the fluorescence recovery of GFP in these conditions is strongly inhibited by the introduction of nanoparticles (Figure 1, trace C). This simple observation confirms that silica nanoparticles interfere in GFP folding and that GFP/HSP_{60+10} is an appropriate system to study the impact of NPs on spontaneous and catalyzed protein folding. Two levels for nanoparticles action can be then envisioned (Figure 1): NPs can act directly on spontaneous folding by trapping unfolded GFP in their denatured state and/or NPs can act indirectly by inhibiting chaperonin catalyzed folding.

Interaction of Unfolded Proteins with NPs. We first analyzed the spontaneous folding of denatured GFP in the presence or in the absence of NPs (Figure 2). The spontaneous folding of dGFP follows a first order kinetic with a kinetic constant k_1 of 0.005 s^{-1} (see SI part B and Figure S1). The

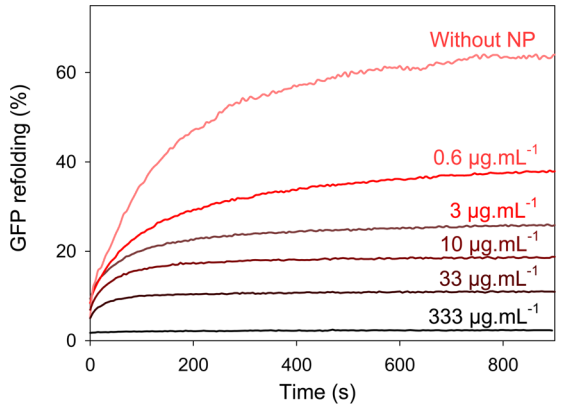

Figure 2. Spontaneous refolding of acid-denatured GFP (1.5 $\mu g\ mL^{-1}$) without NPs and with increasing concentrations of NPs. All experiments were conducted at pH 7.5 in renaturing buffer (25 mM $MgCl_2$, 100 mM KCl, 10 mM Tris-HCl). Data represent the mean of three experiments.

introduction of two equivalent by weight of NPs is sufficient to decrease by 60% the refolding efficiency and no refolding occurs any more for 50 equivalent by weight of NPs.

In order to check whether these observations could be explained by the adsorption of dGFP on silica, we measured the adsorption isotherms of native GFP and dGFP. In this latter case, the isotherm was first measured in denaturing conditions, that is, at pH 1.5, to prevent its refolding during the measurement. We completed this adsorption study by using an irreversibly denatured GFP (idGFP), allowing isotherm measurement in physiological conditions without folding interferences. This idGFP was obtained by aging the protein in its denatured form, which leads to an hysteresis in the refolding process.[15] The adsorbed amounts of these various proteins (Q_{ads}, expressed in mg m^{-2}) as a function of protein concentration in solution (C_{sol}) after adsorption are represented in Figure 3.

GFP does not show any significant adsorption on silica NPs (Figure 3). It could be expected owing to its strong structuration and the presence of the fluorescent aromatic cluster, two structural determinants of protein nonadsorption.[5] Both dGFP and idGFP show a strong adsorption on silica nanoparticles but, contrary to most folded proteins, dGFP and idGFP adsorption isotherms do not follow a Langmuir expression. (eq 1)

$$Q_{abs} = \frac{Q_{max} K_{ads} C_{sol}}{K_{ads} C_{sol} + 1} \quad (1)$$

where Q_{max} is the maximum amount of protein that can be adsorbed on the surface and K_{ads} the adsorption constant.

In order to compare the different systems, we used the more general Langmuir−Freundlich adsorption isotherm to analyze the data (eq 2).[16]

$$Q_{abs} = \frac{Q_{max} (K_{ads} C_{sol})^n}{(K_{ads} C_{sol})^n + 1} \quad (2)$$

where Q_{max} and K_{ads} have the same meaning as in the Langmuir isotherm. The additional parameter n introduces a distribution

DOI: 10.1021/acs.langmuir.5b03890
Langmuir 2016, 32, 195−202

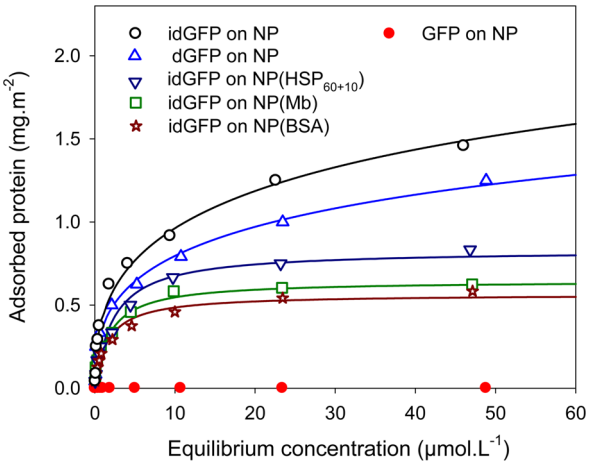

Figure 3. (red ●) Adsorption isotherms of GFP on raw SiO_2 NP in renaturing buffer pH 7.5 (25 mM $MgCl_2$, 100 mM KCl, 10 mM Tris-HCl). (△) Adsorption isotherms of reversibly denatured GFP (dGFP) on raw SiO_2 nanoparticles (40 μg mL^{-1}) at pH 1.5 in 25 mM $MgCl_2$, 100 mM KCl ; Adsorption isotherms of irreversibly denatured GFP (idGFP) in renaturing buffer pH 7.5 respectively on: (○) raw NP (★) BSA-coated nanoparticles (40 μg mL^{-1} in NP, 5 μg mL^{-1} in adsorbed BSA) (□) myoglobin-coated nanoparticles; (40 μg mL^{-1} in NP, 2 μg mL^{-1} in adsorbed Mb) (▽) HSP_{60+10} coated nanoparticles. (40 μg mL^{-1} in NP, 8 μg mL^{-1} in adsorbed HSP_{60+10}). The lines correspond to the adjustment of the data according to eq 2 (see Table 1).

of affinity constants centered on K_{ads}, corresponding to heterogeneous adsorption sites/multilayer formation (the so-called Freundlich behavior). With n = 1, it reduces to the Langmuir isotherm.

Table 1 shows the various parameters obtained by adjusting the data in Figure 3 with eq 2 and compare them with the

Table 1. Parameters of Langmuir Freundlich Model Used for the Fitting of the Adsorption Isotherms: Maximum Amount of Adsorbed Protein (Q_{max}), Adsorption Constant (K_{ads}) and Distribution of Affinity Constants (n) for Each Tested NP/Protein Couple

	Q_{max} (mg m^{-2})	K_{ads} (M^{-1})	n
GFP on NP (a)	nd	10	nd
dGFP on NP	3	8×10^3	0.4
idGFP on NP	3.7	8.1×10^3	0.43
Mb on NP	0.35	7.0×10^4	1
BSA on NP	0.66	3.5×10^5	1
idGFP on NP(BSA)	0.65	5.5×10^5	1
idGFP on NP(Mb)	0.67	6×10^5	1
idGFP on NP(HSP_{60+10})	0.83	4.35×10^5	1

parameters obtained for myoglobin (Mb) and bovine serum albumin (BSA) adsorption on silica nanoparticles.[17] The values of Q_{max} determined for idGFP and dGFP are much higher than the ones measured for folded Mb and BSA whereas the average affinity constants are smaller. This suggests a multilayer adsorption process, the outer layers being more loosely bound than the inner ones. Furthermore, idGFP at pH 7.5 and dGFP at pH 1.5 have very similar adsorption properties. This shows that the adsorption process is not sensitive to protein/silica charges and thus probably driven by hydrophobic interactions.[18] For idGFP and dGFP, the corresponding distribution in adsorption affinity was determined following Umpleby et al.[16] (see Figure S2 and SI part C). For $K_{ads} = 8 \times 10^3$ M^{-1} and $n = 0.4$, 10% of the adsorption sites have an affinity higher than 10^6 M^{-1}, 1 order of magnitude higher than the affinity most often observed in protein adsorption. These high affinity sites may seem scarce, but they still allow the adsorption of 0.30 mg m^{-2} dGFP, which can be compared to the 0.35 mg m^{-2} maximum adsorption of myoglobin on the same surface (Table 1). Furthermore, we must keep in mind that native GFP does not adsorb on silica. Using the high sensitivity of fluorescence measurements, we could determine that only 0.0001 mg m^{-2} adsorbs on NPs from a 5 μM GFP solution. This Q_{ads} and the number of absorption sites on silica for dGFP allow giving a lower value for $K_{ads\text{-}GFP}$ of 10 M^{-1} using eq 1. This means that the denaturation of GFP leads to, at least, a 3 orders of magnitude increase of its K_{ads}.

This increase can be understood from structural and thermodynamic considerations on the adsorption process itself. Most proteins loose some secondary structure upon adsorption. The origin of this destructuration is not completely clear, but it probably allows to optimize the protein surface interactions and to promote water desorption from the surface.[18−20] The main limitation for protein adsorption is the energy required to achieve this partial unfolding. For highly structured proteins such as native GFP, the so-called hard proteins,[18] the destructuration penalty is so high that they do not adsorb. For partially or totally unfolded proteins, this penalty is removed, which in turn corresponds to a considerable gain in affinity. The Gibbs free energy of denaturation of the GFP we used was evaluated to 5 kcal mol^{-1}.[21] Decreasing $\Delta_r G°$ for the adsorption process by this amount corresponds to a 5000 fold increase in K_{ads} upon denaturation, without taking into account the additional interactions that can appear between the surface and the denatured protein. By analogy, we can expect a gain in affinity for surfaces of all proteins upon denaturation.

Beside thermodynamic information, the result presented in Figure 2 allows to determine the adsorption kinetics of denatured GFP, using a simple competition model between folding (eq 3) and adsorption (eq 4) (see SI part D).

$$\text{dGFP} \rightarrow \text{GFP}\ k_1 = 0.005 s^{-1} \quad (3)$$

$$\text{dGFP} + S_{NP} \rightarrow \text{dGFP}_{\text{adsorbed}}\ k_2 = 3.5 \times 10^4\ M^{-1}s^{-1} \quad (4)$$

where S_{NP} is an adsorption site on NP surface.

Within this model, a k_2 constant of 3.5×10^4 L mol^{-1} could be deduced from the dependence of the fluorescence level achieved after refolding in Figure 2 on the concentration of adsorption sites (eq S3 and Figure S4). This corresponds in our conditions to a surface capture of dGFP in the sub second range, obviously much faster than the dGFP folding. We were not able to find any comparative value for the kinetics of protein adsorption on nanoparticles but Docoslis and co-workers determined the kinetic constant of BSA adsorption on silica microparticles in the 10^6 L mol^{-1} s^{-1} range.[22] More data should be gathered on different NP(protein) systems in order to understand the significance of these differences in kinetic constants.

As proteins are expected to cover NPs in physiological conditions and to form the so-called hard corona,[23] we also checked whether the trapping/inhibition of spontaneous folding of dGFP was conserved on NPs already decorated with proteins. First we measured the folding of dGFP in the presence of NPs partially covered with dGFP. As shown in Figure 4, the spontaneous folding of dGFP can be recovered once the half saturation of the surface is reached on the

DOI: 10.1021/acs.langmuir.5b03890
Langmuir 2016, 32, 195−202

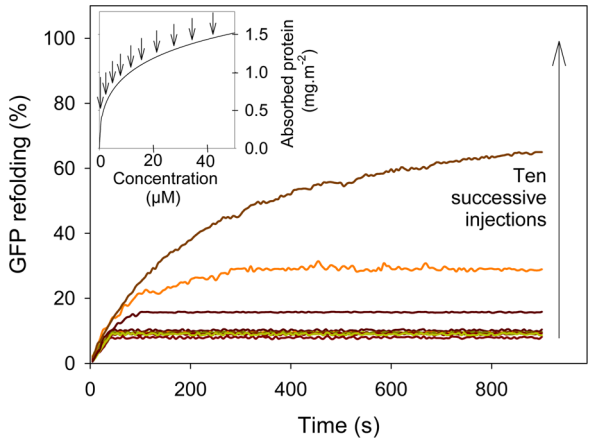

Figure 4. Spontaneous refolding of acid-denatured GFP in the presence of raw SiO_2 nanoparticles (40 μg mL^{-1}) for 10 successive injections of 1 μg mL^{-1} of dGFP. The corresponding points on the dGFP isotherm are shown by arrows in the inset. All experiments were conducted at pH 7.5 in renaturing buffer (25 mM $MgCl_2$, 100 mM KCl, 10 mM Tris-HCl).

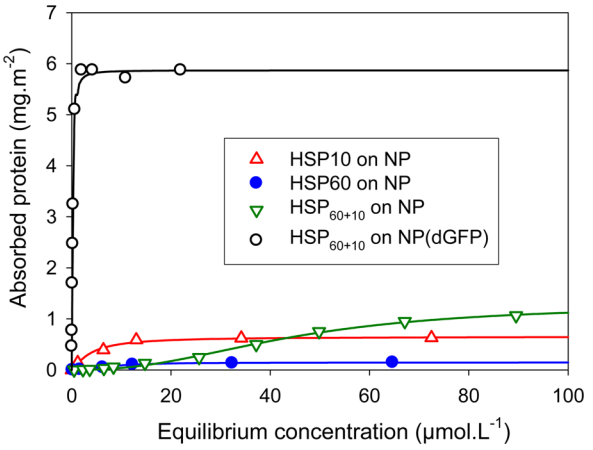

Figure 5. Adsorption isotherms of monomeric HSP10,(△) monomeric HSP60 (blue ●) and of the complex HSP_{60+10} (▽) on raw silica nanoparticles (40 μg mL^{-1}). (○) Adsorption isotherms of the complex HSP_{60+10} on dGFP coated nanoparticles (40 μg mL^{-1} in NP, 10 μg mL^{-1} in adsorbed dGFP). All experiments were conducted at pH 7.5 in renaturing buffer (25 mM $MgCl_2$, 100 mM KCl, 10 mM Tris-HCl). The lines correspond to the adjustment of the data according to eq 2 (see Table 2).

adsorption isotherm. At lower coatings, NP(dGFP) assemblies compete as efficiently as naked NPs with the spontaneous folding.

We checked then whether the dGFP trapping was conserved on NPs decorated with proteins different from dGFP. We were expecting a very strong decrease in idGFP adsorption in these conditions, as proteins are indeed often used to protect surfaces from nonspecific adsorption. However, this conception appeared to be wrong, as idGFP adsorbs on the three tested surfaces, that is, covered by BSA (NP(BSA)), Mb (NP(Mb)) or HSP_{60+10} (NP(HSP_{60+10})) (Figure 3). For all three systems, isotherms follow the Langmuir model and Q_{max} are below 1 mg m^{-2}, suggesting an idGFP adsorption as monolayers on protein-coated NPs. The corresponding K_{ads} are high, in the 10^5 M^{-1} range. For NP(Mb), where the presence of a chromophore allowed the analysis of a potential release of the precoated Mb, we did not observe any Vroman effect.[24] Taken together, these observations show that idGFP sticks on adsorbed proteins. As expected from these sticking properties, BSA-coated NPs also limit the spontaneous folding efficiency of denatured GFP (see SI Figure S5), albeit slightly less efficiently than naked nanoparticles.

Therefore, almost all NP systems tested trap unfolded GFP, the only way to prevent silica surfaces from interfering in spontaneous refolding being to saturate them with denatured proteins.

Functionality of Chaperonin in the Presence of NPs. Prior to complexifying further the NP/dGFP system by adding chaperonins to it, we first analyzed the potential interactions of unassembled and assembled chaperonins with naked nanoparticles. The chaperonin system we used is indeed composed of two components HSP10 and HSP60, which self-assemble in the presence of ATP to form a barrel of 14 units of HSP60 and a lid of seven units of HSP10.[14] It is the assembled $HSP10_7$/$HSP60_{14}$ system that is referred in this document as HSP_{60+10}. We tested the adsorption properties of the two nonfunctional monomers, and the assembled functional HSP_{60+10} on naked silica NPs (Figure 5).

HSP10, HSP60, and HSP_{60+10} follow Langmuir–Freundlich isotherms (eq 2) with n values higher than one (Table 2). Such values sign a cooperative adsorption process,[25] probably due to interactions between adsorbed proteins.

Table 2. Parameters of Langmuir Freundlich Model for the Fitting of the Adsorption Isotherms of HSP Components on NPs: Maximum Amount of Adsorbed Protein (Q_{max}), Adsorption Constant (K_{ads}) and Distribution of Affinity Constants (n)

	Q_{max} (mg m^{-2})	K_{ads} (M^{-1})	n
HSP60 monomers on NP	0.15	1.3×10^5	2.2
HSP10 monomers on NP	0.65	2.7×10^5	1.3
HSP_{60+10} on NP	1.3	2.25×10^4	2.3
HSP_{60+10} on NP(dGFP)	5.9	5×10^6	1.5
HSP_{60+10} on NP(BSA)	$< 10^{-3}$	nd	nd

For HSP monomers, the surface coverage achieved and the adsorption constants are comparable to the one for other globular proteins such as Mb and BSA. For a large complex like HSP_{60+10} (MW > 800 000 Da), we did not find any reference system to compare to. However, the lower affinity and the higher coverage of HSP_{60+10} compared to HSP10 and HSP60 can be explained by the large size of HSP_{60+10}, that increases the corona thickness around the NPs, but decreases the number of protein subunits simultaneously accessible to the NPs.

For HSP_{60+10}, the composition of the protein corona was more precisely analyzed both by denaturing and nondenaturing polyacrylamide gel electrophoresis (SI part F). In denaturing conditions, both HSP60 and HSP10 are identified on the surface (Figure S6). Their concentration ratio is not very different from the initial composition of the solution, even if the concentrated supernatant (line NADS) shows a slight depletion in HSP60 that may indicate a limited enrichment of the surface in this protein.

Non denaturing gel electrophoresis were conducted to characterize the stability of the quaternary structure of HSP oligomers with respect to adsorption (Figure S7). The HSP10 heptamer retains its native quaternary structure after adsorption, while the HSP60 tetradecamer cannot be observed

DOI: 10.1021/acs.langmuir.5b03890
Langmuir 2016, 32, 195–202

because of its high mass. No signature of aggregation or fragmentation of these oligomers was observed neither for HSP10 nor for HSP60.

Since chaperonin appears to be stable upon adsorption on NPs, we analyzed further their folding activity. Figure 6

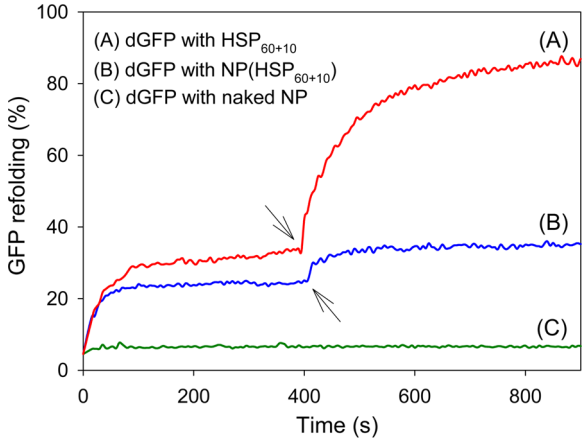

Figure 6. Refolding of acid-denatured GFP (50 nM): (A) in the presence of the HSP_{60+10} complex system (0.2 μM); (B) in the presence of the HSP_{60+10} complex absorbed on nanoparticles (1 mg mL^{-1} in silica NP, 0.2 mg mL^{-1} in absorbed HSP_{60+10}); (C) in the presence of raw SiO_2 nanoparticles (1 mg mL^{-1}). The arrows show the addition time of ATP (1 mM) to HSP_{60+10} containing solutions. All experiments were conducted at pH 7.5 in renaturing buffer (25 mM $MgCl_2$, 100 mM KCl, 10 mM Tris-HCl).

presents the fluorescence recovery of dGFP in the presence of free and NP bound HSP_{60+10} (and in the presence of same amount of naked NPs as a reminder). The renaturation curve with free HSP_{60+10} present two parts (Figure 6A): the first part corresponds to the competition between the spontaneous folding of dGFP and its trapping by HSP systems (called here T phase); the second part corresponds to the catalyzed folding of the trapped GFP that is triggered by the introduction of ATP (called C phase). The refolding in the C phase occurs with a typical catalytic constant of 0.009 s^{-1} (see SI part B and Figure S2), comparable to the one measured in the literature for HSP_{60+10}.[26] We must notice that a low fluorescence recovery in the T phase corresponds here to an efficient trapping by HSP, whereas a high fluorescence recovery in the C phase corresponds to an efficient catalytic step.

When dGFP is exposed to HSP_{60+10} preadsorbed on NPs (Figure 6B), the catalytic phase almost disappears while the trapping phase is not significantly modified with respect to Figure 6A. Compared to naked nanoparticles (Figure 6C), the persistence of a T phase in Figure 6B similar to one of nonadsorbed HSP_{60+10} suggests: (i) that adsorbed HSP_{60+10} protects partially dGFP from trapping on NPs (ii) that adsorbed HSP_{60+10} keeps its own dGFP trapping capability. However, the disappearance of a real C phase in Figure 6B shows that adsorbed HSP_{60+10} is not able to complete the refolding processes.

We finally analyzed the behavior of HSP_{60+10} complexes in the presence of NPs precoated either by native BSA or by denatured GFP.

HSP_{60+10} did not show any significant adsorption on NP(BSA) (see SI Figure S8 and Table 2). This result is per se interesting, as most soft proteins like BSA unfold partially upon adsorption,[27] thus raising the question of the interaction of these unfolded states with the protein reparation machinery. BSA adsorption does not lead to the apparition of chaperonin recognition sites. Still the effect of NP(BSA) on HSP_{60+10} catalyzed dGFP refolding was difficult to predict. On the one hand, the nonadsorption of HSP_{60+10} could preserve their activity. On the other hand, the dGFP adsorption on NP(BSA) (Figure 3) could prevent their loading into HSP's cavity. The refolding experiment shows in Figure 7 a limited effect of

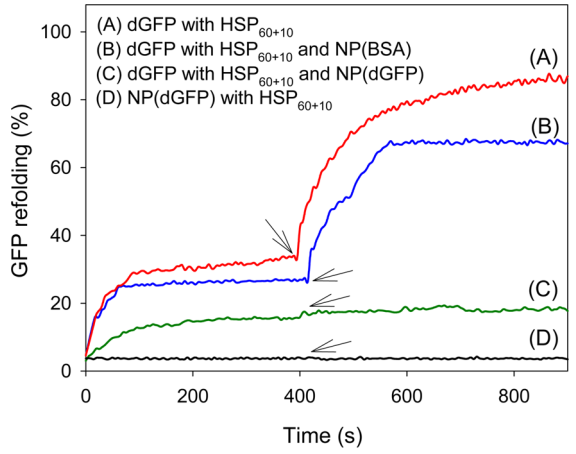

Figure 7. Refolding of acid-denatured GFP (50 nM): (A) in the presence of the HSP_{60+10} complex system (0.2 μM); (B) in the presence of the HSP_{60+10} complex system (0.2 μM) and of BSA covered NP (1 mg mL^{-1} in NP, 0.12 mg mL^{-1} in adsorbed BSA); (C) in the presence of the HSP_{60+10} complex system (0.2 μM) and of dGFP covered silica nanoparticles (1 mg mL^{-1} in NP, 0.25 mg mL^{-1} in adsorbed dGFP). (D) Behavior of preadsorbed dGFP (40 μg mL^{-1} in NP, 10 μg mL^{-1} in adsorbed dGFP) in the presence of the HSP_{60+10} complex system (0.2 μM). The arrows show the addition time of ATP (1 mM). All experiments were conducted at pH 7.5 in renaturing buffer (25 mM $MgCl_2$, 100 mM KCl, 10 mM Tris-HCl).

NP(BSA) on the HSP_{60+10} trapping and catalytic activities (Figure 7B compared to Figure 7A) suggesting that the dGFP affinity for NP(BSA) surface is not sufficient to prevent its handling by chaperonins.

Contrary to NP(BSA), dGFP coated NPs show a very strong affinity for HSPs, in the 10^6 M^{-1} range (see Table 2 and Figure 5) and can bind up to 6 mg m^{-2} of protein. This phenomenon seems specific of the dGFP/HSP_{60+10} couple, as it is not found for HSP_{60+10} on NP(BSA) and is very limited for BSA on NP(dGFP) (Table 2 and Figure S8 in SI).

Figure 7D shows that, despite this affinity, dGFP adsorbed on nanoparticles cannot be rescued by HSPs. Furthermore, the folding catalytic activity of HSP_{60+10} with respect to free dGFP disappears in the presence of NP(dGFP) (Figure 7C compared to Figure 7A). We must notice that, even if HSP_{60+10} are inhibited by nanoparticles covered by unfolded GFP, the dGFP trapping capability of HSP_{60+10}/NP(dGFP) mixtures (see the T phase of Figure 7C) is more pronounced than the one of HSP_{60+10} (Figure 7A) or of NP(dGFP) (see the last curve of Figure 4) alone. We can infer that NP(dGFP) are recognized as substrates by the HSPs, that this recognition inhibits HSP_{60+10} folding function but does not saturate dGFP binding sites.

Discussion: Biological Implications of Our Observations. We had two initial questions: can unfolded proteins stick to NPs ? If so, can this phenomenon perturb chaperonin systems? The answer to both is positive. Furthermore, the combined affinities of unfolded proteins toward NPs and of

DOI: 10.1021/acs.langmuir.5b03890
Langmuir 2016, 32, 195−202

chaperonins toward adsorbed unfolded proteins are probably sufficient to explain the overrepresentation of chaperonins in the NPs' corona evidenced by the proteomic studies cited in the introduction.

We must notice that the fact that unfolded proteins are more prone to adsorption than folded ones was not completely unexpected. It is well-known that surface fouling, especially in the food industries, is much more pronounced at higher temperature, and that, more generally, most denaturing treatments make proteins "sticky".[28] Our observations provide a quantitative description for this phenomenon, showing that denatured proteins behave quite differently from folded proteins with respect to surfaces. Unfolded proteins adsorb with a higher coverage and more heterogeneous interactions, with some high affinity sites. Moreover, they can adsorb on surfaces already covered by proteins. These original properties arise probably from the diversity of side-chains and conformations unfolded proteins can present that allow them to optimize their interaction with surfaces in a combinatorial fashion.

These observations also suggest that all unfolded proteins, and especially proteins during their elongation step, may be a biological target for NPs, but do not indicate whether relevant concentrations in NPs can interfere in the cytoplasm with the de novo folding or with the refolding of proteins. We must first notice that most NP concentrations we used here are realistic, as bioaccumulation studies have demonstrated concentrations in NPs as high as 100 μg mL^{-1} were achieved for many days in rat liver.[29] We choose a conservative value of 10 μg mL^{-1} in this discussion.

The question of the in vivo impact of NPs on the refolding of stressed proteins by HSPs has two aspects. The first one is HSP sequestration by NPs: as HSPs are very abundant proteins (a few mg mL^{-1})[30] we do not expect any effect of sequestration on the overall HSP folding activity. The second one is the competition between NPs and HSPs for unfolded proteins. Even though, owing to their concentration, HSP_{60+10} are expected to capture unfolded proteins at a higher speed than NPs, competition kinetics predicts that a significant percentage of stress unfolded proteins will be trapped by NPs (see SI part H).

The question of the impact on the spontaneous folding of neosynthesized protein is more delicate to answer. Some authors evaluate the time a protein remains unfolded to a few seconds, the time needed to produce the 4−6 amino acid required to form a secondary structure.[31] Applying the competition kinetics described above, and taking k = 0.1 s^{-1} for the in vivo folding rate, 10 μg mL^{-1} of nanoparticles would be capable to capture 5% of the newly synthesized proteins (SI part H). This does not seem critical for the most abundant proteins (mostly involved in metabolism), but may be crucial for proteins with low copy numbers (usually involved in regulation processes[32]) if they happen to be in the captured pool. On the other hand, these phenomena would have a limited extension in time as they could lead to a saturation of NPs with unfolded polypeptides within hours.

These various remarks lead to a common conclusion: silica NPs can probably store some -but not all- unfolded proteins. This raises the (final) question of the putative toxicity of the nanoparticle/unfolded proteins assembly. Such assemblies share a number of characteristics with so-called "small disordered aggregates of proteins", that are known to be highly toxic due to the interaction of the misfolded proteins on their surfaces with cell membranes.[33] Therefore, we can only suggest to give a detailed look at the capability of unfolded protein covered NPs to affect membranes' integrity. We must finally notice that our observations apply only to the competition between the folding processes and surface adsorption. Further studies will be required to connect these results to the known capabilities of NPs to favor or inhibit unfolded protein fibrillation/aggregation.[34]

CONCLUSIONS

GFP denaturation leads to an important increase of its affinity toward silica surface. This affinity explains why silica nanoparticles show, with respect both to GFP spontaneous and catalyzed folding, an antichaperonin activity, in the sense that (i) they efficiently trap and stabilize proteins in their unfolded state and (ii) they trap and inhibit chaperonins when covered by unfolded proteins.

EXPERIMENTAL SECTION

Protein Preparation. The GFP and the monomeric forms of HSP60 and HSP10 were expressed and purified, while the active form of the proteic complex HSP_{60+10} (Chaperonin60:Chaperonin10, 1:1; overexpressed in *E. coli*; ref 030M4060), myoglobin (Myoglobin from equine heart, ref M18888), BSA (Albumin from bovine serum, ref A7030) and Mg-ATP (ref A9187) were purchased from Sigma-Aldrich in dry conditioning and purity >95%.

We used a GFP variant, GFP-F64L/S65T also known as EGFP, fused with polyhistidine (HisX6) at its NH_2-terminus and expressed in *Escherichia coli* XL-1 Blue cells. It will be designed hereater as GFP. GFP gene was cloned in pQE32 plasmids according to standard protocols. The recombinant GFP was purified by Ni-affinity chromatography (Ni-Sepharose 6 Fast Flow, ref 17-0756-01, GE Healthcare, Bio-Sciences AB, Sweden) in pH 7.5 Tris-HCl buffer (Trizma Base, ref T6066, Sigma-Aldrich). Proteins eluted from the affinity beads were judged to be >97% pure by Coomassie-stained (Brilliant Blue G-250, ref B1131, Sigma-Aldrich) sodium dodecyl sulfate polyacrylamide gel Electrophoresis (SDS-PAGE). Protein concentration was determined by the Bradford method (Protein Assay Dye Reagent Concentrate, ref 500-0006, Bio-Rad) and by UV/visible spectroscopy at 280 and 488 nm using the calculated molar absorptivity 20 010 and 55 000 M^{-1} cm^{-1} respectively.[35]

To express and purify the chaperone monomers, we used a published expression,[36,37] where HSP60 and HSP10 genes were cloned in a high-copy URA3 expression vector (pEG(KG)). The proteins were fused to glutathione S-tranferase polyhistidine (GST-HisX6) at their NH_2-termini and expressed in yeast (*Saccharomyces cerevisiae* BY4741 Mat A) using the inducible GAL1 promoter. For preparing samples, we grew cells (200 mL) in medium containing raffinose (final concentration 4%) to O.D.(600) ∼ 0.8 in Erlenmeyer. Galactose was added to a final concentration of 4% to induce protein expression, and the cells were incubated for 4 h. The cultures were washed once with 4 °C sterile MilliQ water, resuspended in 2.5 mL chilled lysis buffer (Dubelcco's PBS 1X, ref.D1408, Sigma-Aldrich; phenylmethylsulfonyl fluoride 1 mM, ref 36978, Thermo Fisher Scientific Inc.; Halt Protease inhibitor Cocktail 1X, ref.78429, Thermo Fisher Scientific Inc.) and transferred into a French press cell (5 mL) frozen at −75 °C in an ethanol/dry ice bath. After 1 h of incubation in −75 °C bath, cells were lysed by applying 6 × 10^5 Pa with the French press (Rassant Truck Tech PRM12, France). The cell lysate was collected and allowed to defrost but kept at 4 °C on ice. Cells debris were removed by centrifugation at 4 °C for 45 min at 20,000 g. The GST-HisX6 fusion proteins were purified from the lysate supernatant using two-step affinity chromatography with glutathione (Glutathione SepharoseTM 4B, ref 17-0756601, GE Healthcare, Bio-Sciences AB, Sweden) and Ni-NTA beads according to standard protocols in batch. The quality and quantity of the purified proteins (HSP60 and HSP10) were monitored by SDS-PAGE and Western blotting using anti-

DOI: 10.1021/acs.langmuir.5b03890
Langmuir 2016, 32, 195−202

polyHis antibodies (Monoclonal mouse Anti·His Antibodies, ref 34698, Qiagen). The results indicated that the purified proteins are more than 95% pure. Finally concentrations were determined by the Bradford method and by UV spectroscopy at 280 nm using the calculated molar absorptivity HSP60 = 10 550 M^{-1} cm^{-1} and HSP10 = 1490 M^{-1} cm^{-1}.[38]

Spectroscopic Measurements. Fluorescence spectra were recorded on a Fluoromax-4 (Horiba, Kyoto, Japan). Excitation and emission monochromator slit widths were 2 nm. Fluorescence data were corrected for background and dilution. All measurements were performed at 25 °C, which is the optimal temperature for HSP complexes activity. Emission was recorded at 508 nm, while the excitation was set at 470 nm.

Silica Nanoparticles Characterization. The silica nanoparticles used (99.5% purity, Sigma-Aldrich ref 637238) have been extensively characterized previously.[5] The NP specific surface measured by gas adsorption is 170 m^2 g^{-1}. NP size and shape were characterized by transmission electron microscopy and small-angle neutron scattering. The major particle population is composed of spherical objects with a mean diameter of 26 ± 2 nm. In aqueous solution, the NPs tend to form small aggregates of a mean size of 50 nm. For all experiments NPs were prepared freshly in Tris-HCl buffer (pH 7.5) at the final concentration of 25 g L^{-1}. In these conditions, the nanoparticles are negatively charged (Zeta potential of −20 mV).

Adsorption and Adsorption Isotherms. *Generals.* Adsorption isotherms represent the adsorbed proteins amounts versus proteins concentration in solution. Samples with protein concentration ranging from 1 to 50 μM in 10 mM Tris-HCl buffer were divided into two sets: one with proteins only for reference and a second with NPs at 40 μg mL^{-1}. Both sets were gently agitated 3 h at room temperature and then centrifuged at 17 000*g* for 10 min. Protein concentrations were measured in supernatant by UV/vis spectroscopy and the concentration of adsorbed proteins was calculated as the difference between concentrations of the two sets, with and without NPs. Adsorbed proteins amounts were expressed in mg m^{-2}, based on NP active surface area previously measured. An uncertainty of 5% was determined by repeating 3 times these experiments.

Adsorption on Protein Covered Nanoparticles. To perform multilayers adsorption experiments on NPs, each sublayer was constructed by exposing NPs for 3h to a saturating protein solution. Saturation concentrations of protein used were defined according to adsorption isotherms determined in single layer conditions (see above, adsorption were conducted in acidic conditions for dGFP). The saturated NPs were collected by centrifugation (10 min; 17 000*g*; ambient temperature) and resuspended in 10 mM Tris-HCl by a gentle agitation. Theses NPs were then used for experiments on the outermost layer in terms of adsorption isotherms with a different protein and of activity if HSP were to be tested. During these latter experiments, the eventual protein desorption from the underlying layer was followed by UV−visible spectroscopy (for myoglobin ε_{623} = 3500 M^{-1} cm^{-1};[39] for GFP ε_{488} = 55,000 M^{-1} cm^{-1}[35]) or fluorescence.

Denaturation and Refolding of GFP. Refolding analysis of acid-denatured GFP was performed in presence or not of chaperone and/or nanoparticles. GFP folding were carried out at 25 °C. We confirmed that GFP can fold efficiently from an acid-denatured state as reported by Ward and Bookman.[40] We used acid-denaturation instead of base- or guanidine-HCl-denaturation to avoid confusion caused from transient formation of other fluorescent species at alkaline pH and from the effect of residual guanidine-HCl in the diluted solution. For experiments 10 μM GFP solution (10 mM Tris-HCl, pH7.5) was mixed with the same volume of 125 mM HCl (min 37%, ref 30-721, Riedel-de Haën) and incubated 1 min to give denatured GFP (dGFP) solution (final 5 μM, pH 1.5). dGFP was 100-fold diluted into a dilution buffer (25 mM $MgCl_2$,$6H_20$, ref 104-20, Sigma-Aldrich ; 100 mM KCl, ref P3911, Sigma-Aldrich ; 10 mM Tris-HCl) containing no other reagent or containing the HSP complex with or without nanoparticles (final concentration 0.05 μM GFP). We used two forms of dGFP, a reversibly denatured form when dGFP was freshly produced and an irreversibly denatured form when dGFP was conserved at −20 °C for 96h (idGFP). idGFP was dialyzed against 10 mM Tris-HCL pH 7.5 for 2 days at 4 °C to increase the pH from 1.5 to 7.5 for adsorption studies. We checked that our denaturation conditions lead to a total unfolding of the proteins (see circular dichroism in SI part I).

Spontaneous folding of reversible dGFP started upon 100 times dilution of a 5 μM stock solution into 10 mM Tris-HCl, pH 7.5 without chaperone or nanoparticles. When chaperonin was present in the buffer (0.2 μM), dGFP was trapped, and folding was suppressed.[13] 400 s after the dilution time, Mg-ATP (1 mM final concentration) was added to resume folding. Generation of the fluorescence at 508 nm by excitation light at 470 nm was monitored continuously with a fluorometer (Fluoromax-4, Horiba). As a control, native GFP was diluted 100-fold into the same dilution buffer, and the fluorescence was measured. The fluorescence intensity of the native GFP was not influenced by the dilution buffer or the presence of HSP complexes, and its value was taken as reference. In the case of experiments with nanoparticles we verified that raw and saturated nanoparticles did not interfere with GFP fluorescence.

Data Analysis. Kinetic data and isotherms were adjusted using non linear least-squares fitting on Excel.[41]

■ ASSOCIATED CONTENT

Supporting Information

The Supporting Information is available free of charge on the ACS Publications website at DOI: 10.1021/acs.langmuir.5b03890.

Proteomic data, spontaneous and catalyzed refolding kinetics, competition of NPs for unfolded protein capture, additional refolding curves, additional isotherms, distribution of K values in Langmuir−Freundlich isotherms, gel electrophoresis of adsorbed HSP_{60+10}, circular dichroism spectra of acid-denatured GFP (PDF)

■ AUTHOR INFORMATION

Corresponding Author

*E-mail: jprenault@cea.fr.

Notes

The authors declare no competing financial interest.

■ ACKNOWLEDGMENTS

We acknowledge support from the "programme de Toxicologie" of the CEA. The GFP plasmid was a kind gift from Stéphane Chédin and Jean Yves Thuret. We thank Laurent Marichal for carefully reading the manuscript.We acknowledge also SOLEIL for provision of synchrotron radiation facilities and we would like to thank Frank Wien for assistance in using the DISCO beamline.

■ REFERENCES

(1) Sanhai, W. R.; Sakamoto, J. H.; Canady, R.; Ferrari, M. Seven challenges for nanomedicine. *Nat. Nanotechnol.* **2008**, *3* (5), 242−244.

(2) (a) Monopoli, M. P.; Aberg, C.; Salvati, A.; Dawson, K. A. Biomolecular coronas provide the biological identity of nanosized materials. *Nat. Nanotechnol.* **2012**, *7* (12), 779−786. (b) Lesniak, A.; Fenaroli, F.; Monopoli, M. R.; Aberg, C.; Dawson, K. A.; Salvati, A. Effects of the presence or absence of a protein corona on silica nanoparticle uptake and impact on cells. *ACS Nano* **2012**, *6* (7), 5845−5857.

(3) (a) Johnson, B. J.; Russ Algar, W.; Malanoski, A. P.; Ancona, M. G.; Medintz, I. L. Understanding enzymatic acceleration at nanoparticle interfaces: Approaches and challenges. *Nano Today* **2014**, *9* (1), 102−131. (b) Mahmoudi, M.; Lynch, I.; Ejtehadi, M. R.; Monopoli, M. P.; Bombelli, F. B.; Laurent, S. Protein−Nanoparticle Interactions: Opportunities and Challenges. *Chem. Rev.* **2011**, *111* (9), 5610−5637. (c) Mu, Q.; Jiang, G.; Chen, L.; Zhou, H.; Fourches, D.;

DOI: 10.1021/acs.langmuir.5b03890
Langmuir 2016, 32, 195−202

Tropsha, A.; Yan, B. Chemical Basis of Interactions Between Engineered Nanoparticles and Biological Systems. *Chem. Rev.* **2014**, *114* (15), 7740−7781.
(4) Lai, Z. W.; Yan, Y.; Caruso, F.; Nice, E. C. Emerging Techniques in Proteomics for Probing Nano−Bio Interactions. *ACS Nano* **2012**, *6* (12), 10438−10448.
(5) Mathe, C.; Devineau, S.; Aude, J.-C.; Lagniel, G.; Chedin, S.; Legros, V.; Mathon, M.-H.; Renault, J.-P.; Pin, S.; Boulard, Y.; Labarre, J. Structural Determinants for Protein adsorption/non-adsorption to Silica Surface. *PLoS One* **2013**, *8* (11), e81346.
(6) Saibil, H. Chaperone machines for protein folding, unfolding and disaggregation. *Nat. Rev. Mol. Cell Biol.* **2013**, *14* (10), 630−642.
(7) Macario, A. L.; Conway de Macario, E.; Cappello, F. *The Chaperonopathies*; Springer: Netherlands, 2013.
(8) Auluck, P. K.; Chan, H. Y. E.; Trojanowski, J. Q.; Lee, V. M. Y.; Bonini, N. M. Chaperone suppression of alpha-synuclein toxicity in a Drosophila model for Parkinson's disease. *Science* **2002**, *295* (5556), 865−868.
(9) Whitesell, L.; Lindquist, S. L. HSP90 and the chaperoning of cancer. *Nat. Rev. Cancer* **2005**, *5* (10), 761−772.
(10) Moos, P. J.; Olszewski, K.; Honeggar, M.; Cassidy, P.; Leachman, S.; Woessner, D.; Cutler, N. S.; Veranth, J. M. Responses of human cells to ZnO nanoparticles: a gene transcription study. *Metallomics* **2011**, *3* (11), 1199−1211.
(11) Makumire, S.; Revaprasadu, N.; Shonhai, A., DnaK Protein alleviates toxicity induced by citrate-coated gold nanoparticles in Escherichia coli. *PLoS One* **2015**, *10* (4), e012124310.1371/journal.-pone.0121243
(12) Yang, X.; Liu, J.; He, H.; Zhou, L.; Gong, C.; Wang, X.; Yang, L.; Yuan, J.; Huang, H.; He, L.; Zhang, B.; Zhuang, Z. SiO(2)-nanoparticles induce cytotoxicity and protein expression alteration in HaCaT cells. *Part. Fibre Toxicol.* **2010**, *7*, 1−1.
(13) Makino, Y.; Amada, K.; Taguchi, H.; Yoshida, M. Chaperonin-mediated Folding of Green Fluorescent Protein. *J. Biol. Chem.* **1997**, *272* (19), 12468−12474.
(14) Hartl, F. U.; Bracher, A.; Hayer-Hartl, M. Molecular chaperones in protein folding and proteostasis. *Nature* **2011**, *475* (7356), 324−332.
(15) Andrews, B. T.; Gosavi, S.; Finke, J. M.; Onuchic, J. N.; Jennings, P. A. The dual-basin landscape in GFP folding. *Proc. Natl. Acad. Sci. U. S. A.* **2008**, *105* (34), 12283−12288.
(16) Umpleby, R. J.; Baxter, S. C.; Chen, Y.; Shah, R. N.; Shimizu, K. D. Characterization of Molecularly Imprinted Polymers with the Langmuir−Freundlich Isotherm. *Anal. Chem.* **2001**, *73* (19), 4584−4591.
(17) Isotherms not shown.
(18) Norde, W. My voyage of discovery to proteins in flatland··· and beyond. *Colloids Surf., B* **2008**, *61* (1), 1−9.
(19) Devineau, S.; Zanotti, J.-M.; Loupiac, C.; Zargarian, L.; Neiers, F.; Pin, S.; Renault, J. P. Myoglobin on Silica: A Case Study of the Impact of Adsorption on Protein Structure and Dynamics. *Langmuir* **2013**, *29* (44), 13465−13472.
(20) Pan, H.; Qin, M.; Meng, W.; Cao, Y.; Wang, W. How Do Proteins Unfold upon Adsorption on Nanoparticle Surfaces? *Langmuir* **2012**, *28* (35), 12779−12787.
(21) Stepanenko, O. V.; Verkhusha, V. V.; Kazakov, V. I.; Shavlovsky, M. M.; Kuznetsova, I. M.; Uversky, V. N.; Turoverov, K. K. Comparative Studies on the Structure and Stability of Fluorescent Proteins EGFP, zFP506, mRFP1, "dimer2", and DsRed1. *Biochemistry* **2004**, *43* (47), 14913−14923.
(22) (a) Docoslis, A.; Wu, W.; Giese, R. F.; van Oss, C. J. Measurements of the kinetic constants of protein adsorption onto silica particles. *Colloids Surf., B* **1999**, *13* (2), 83−104. (b) Jennissen, H. P.; Zumbrink, T. A novel nanolayer biosensor principle. *Biosens. Bioelectron.* **2004**, *19* (9), 987−997.
(23) Lundqvist, M.; Stigler, J.; Elia, G.; Lynch, I.; Cedervall, T.; Dawson, K. A. Nanoparticle size and surface properties determine the protein corona with possible implications for biological impacts. *Proc. Natl. Acad. Sci. U. S. A.* **2008**, *105* (38), 14265−14270.
(24) Vroman, L.; Adams, A.; Fischer, G.; Munoz, P. Interaction of high molecular weight kininogen, factor XII, and fibrinogen in plasma at interfaces. *Blood* **1980**, *55* (1), 156−159.
(25) (a) Jiang, W.; Hearn, M. T. W. Protein Interaction with Immobilized Metal Ion Affinity Ligands under High Ionic Strength Conditions. *Anal. Biochem.* **1996**, *242* (1), 45−54. (b) Sharma, S.; Agarwal, G. P. Interactions of Proteins with Immobilized Metal Ions: A Comparative Analysis Using Various Isotherm Models. *Anal. Biochem.* **2001**, *288* (2), 126−140.
(26) Murai, N.; Taguchi, H.; Yoshida, M. Kinetic Analysis of Interactions between GroEL and reduced α-Lactalbumin: effect of GroES and nucleotides. *J. Biol. Chem.* **1995**, *270* (34), 19957−19963.
(27) Norde, W.; Favier, J. P. Structure of adsorbed and desorbed proteins. *Colloids Surf.* **1992**, *64* (1), 87−93.
(28) (a) Nakanishi, K.; Sakiyama, T.; Imamura, K. On the adsorption of proteins on solid surfaces, a common but very complicated phenomenon. *J. Biosci. Bioeng.* **2001**, *91* (3), 233−244. (b) Czeslik, C., Factors Ruling Protein Adsorption. In *Z. Phys. Chem.*, **2004**, *218*, 771, 10.1524/zpch.218.7.771.35722
(29) Malfatti, M. A.; Palko, H. A.; Kuhn, E. A.; Turteltaub, K. W. Determining the Pharmacokinetics and Long-Term Biodistribution of SiO2 Nanoparticles In Vivo Using Accelerator Mass Spectrometry. *Nano Lett.* **2012**, *12* (11), 5532−5538.
(30) Nagaraj, N.; Wisniewski, J. R.; Geiger, T.; Cox, J.; Kircher, M.; Kelso, J.; Pääbo, S.; Mann, M. Deep proteome and transcriptome mapping of a human cancer cell line. *Mol. Syst. Biol.* **2011**, *7*, 548−548.
(31) Hartl, F. U.; Hayer-Hartl, M. Converging concepts of protein folding in vitro and in vivo. *Nat. Struct. Mol. Biol.* **2009**, *16* (6), 574−581.
(32) Beck, M.; Schmidt, A.; Malmstroem, J.; Claassen, M.; Ori, A.; Szymborska, A.; Herzog, F.; Rinner, O.; Ellenberg, J.; Aebersold, R. The quantitative proteome of a human cell line. *Mol. Syst. Biol.* **2011**, *7* (1), 549.
(33) Bucciantini, M.; Giannoni, E.; Chiti, F.; Baroni, F.; Formigli, L.; Zurdo, J.; Taddei, N.; Ramponi, G.; Dobson, C. M.; Stefani, M. Inherent toxicity of aggregates implies a common mechanism for protein misfolding diseases. *Nature* **2002**, *416* (6880), 507−511.
(34) (a) De, M.; Rotello, V. M. Synthetic "chaperones": nanoparticle-mediated refolding of thermally denatured proteins. *Chem. Commun.* **2008**, *30*, 3504−3506. (b) Mahmoudi, M.; Kalhor, H. R.; Laurent, S.; Lynch, I. Protein fibrillation and nanoparticle interactions: opportunities and challenges. *Nanoscale* **2013**, *5* (7), 2570−2588.
(35) McRae, S. R.; Brown, C. L.; Bushell, G. R. Rapid purification of EGFP, EYFP, and ECFP with high yield and purity. *Protein Expression Purif.* **2005**, *41* (1), 121−127.
(36) Zhu, H.; Klemic, J. F.; Chang, S.; Bertone, P.; Casamayor, A.; Klemic, K. G.; Smith, D.; Gerstein, M.; Reed, M. A.; Snyder, M. Analysis of yeast protein kinases using protein chips. *Nat. Genet.* **2000**, *26* (3), 283−289.
(37) Zhu, H.; Bilgin, M.; Bangham, R.; Hall, D.; Casamayor, A.; Bertone, P.; Lan, N.; Jansen, R.; Bidlingmaier, S.; Houfek, T.; Mitchell, T.; Miller, P.; Dean, R. A.; Gerstein, M.; Snyder, M. Global analysis of protein activities using proteome chips. *Science* **2001**, *293* (5537), 2101−2105.
(38) Cheng, M. Y.; Hartl, F. U.; Norwich, A. L. The mitochondrial chaperonin hsp60 is required for its own assembly. *Nature* **1990**, *348* (6300), 455−458.
(39) Antonini, E. Hemoglobin and Myoglobin in their reactions with ligands. In *Frontiers of Biology*; North Holland Pub. Co.: New York, 1971; Vol. *21*.
(40) Ward, W. W.; Bokman, S. H. Reversible denaturation of aequorea green-fluorescent protein-physical separation and characterization of the renatured protein". *Biochemistry* **1982**, *21* (19), 4535−4540.
(41) Kemmer, G.; Keller, S. Nonlinear least-squares data fitting in Excel spreadsheets. *Nat. Protoc.* **2010**, *5* (2), 267−281.

DOI: 10.1021/acs.langmuir.5b03890
Langmuir 2016, 32, 195−202